This article has been accepted for publication in a future issue of this journal, but has not been fully edited. Content may change prior to final publication. Citation information: DOI 10.1109/LAWP.2016.2536735, IEEE Antennas and Wireless Propagation Letters

A Novel Differentially Fed Compact Dual-Band Implantable Antenna for Biotelemetry Applications

Yijun Liu, Yifan Chen, Haili Lin, and Filbert H. Juwono

***Abstract*—A novel differentially fed dual-band planar antenna operating at the medical implant communication service (MICS) band (402-405 MHz) and the industrial, scientific and medical (ISM) band (2400-2480 MHz) is presented. The measured 10-dB differential reflection coefficient bandwidth is 389-419 MHz (7.4%) at the lower band and 2395-2563 MHz (6.6%) at the upper band, respectively. With the use of symmetric meandered strip and shorting pin, a differentially fed compact dual-band design is obtained, where the volume of the prototype is only 642.62 mm^3 (22mm×23mm×1.27mm). Due to its small size and dual-band operation, the proposed antenna can be connected to differential circuits in implantable biotelemetric devices.**

***Index Terms*—Compact antenna, differentially fed, dual-band, meandered strip, implantable, biotelemetry**

I. Introduction

Recently, implantable microsystems have received increasing attention for applications in biotelemetry [1]-[3]. It is desirable to integrate single antenna with a monolithic radio frequency (RF) front end, which is often constructed by using differential topology. With the use of differential antennas, baluns will no longer be necessary as the differential signals can be directly fed into the antennas. The differential antennas not only work as radiators but also as matching networks and power dividers [4]. As a result, compact and differential antennas for implantable devices are demanded.

A differentially fed dual-band implantable antenna has been reported in [5] for the first time. However, the two resonant frequencies in [5] are 433.9 MHz and 542.4 MHz, both of which are very close to the medical implant communication service (MICS) band. A differentially fed dual-band antenna operating at both the 402-405 MHz MICS band and the 2400-2480 MHz industrial, scientific and medical (ISM) band has been proposed in [6]. The proposed antenna can be wrapped to put in a capsule, thus the size of the implant is very small. However, the designs have no ground plane to prevent the backward radiation, which is harmful for human health. A wideband differential loop-fed patch antenna is implanted in head [7], just only covers single band.

In this paper, a differentially fed compact dual-band implantable antenna with ground plane is developed for near-field biotelemetry applications. By using the symmetric meandered strip and shorting pin, this differentially fed antenna can be integrated into differential RF front end easily without balun and matching circuit. With a ground plane, the smaller backward radiation can reduce any harmful effect caused to the human body. These designs are novel and have not been presented in the existing literatures [2], [5]-[7]. The measured 10-dB bandwidth is 389-419 MHz (7.4%) and 2395-2563 MHz (6.6%), respectively. The simulated 1-g averaged specific absorption rates (SAR) comply with the limitation imposed by the ANSI/IEEE regulation for short-distance biotelemetry [10].

The paper is organized as follows. In Section II, the design of the differentially fed antenna is presented. In Section III, the measurement results of the fabricated antenna are provided and compared against the simulated data. Finally, some concluding remarks are summarized in Section IV.

II. Antenna Design

The geometry of the proposed antenna is depicted in Fig. 1, which has a dimension of 22mm×23mm×1.27mm. All the slots between the strips are 0.5 mm wide. Both the substrate and the superstrate use Rogers 3010 (ε_r=10.2, $\tan\delta$=0.0023) with a thickness of 0.635 mm. The superstrate is necessary to protect the strip from direct contact with the semiconducting bio-fluid. During HFSS simulation, the antenna was placed at 4 mm depth inside a skin-mimicking material with a volume of 1000 mL. The recipe of the skin-mimicking material is 56.18% sugar, 2.33% salt, and 41.49% deionized water for the MICS band, and 53% sugar and 47% deionized water for the ISM band [2]. The measured dielectric properties of the skin-mimicking material are frequency-dependent as shown in Fig. 2, where ε_r=45.97, σ=0.57 S/m at the MICS band and ε_r=36.25, σ=2.46 S/m at the ISM band, respectively. The antenna structure is symmetrical about the line UU′ being the symmetry axis. The meandered strip F-L (dashed line in Fig. 1) with shorting pin is used to obtain broad bandwidth at the MICS band, while the strip F-H (dotted line in Fig. 1) is used to excite resonance at the ISM band. A pair of symmetrical notches NS with dimension of 1.0mm×1.0mm in the two symmetrical strips F-L lengthens the current path at the MICS band. Furthermore, a pair of symmetrical slots SL in the two symmetrical strips F-H

Manuscript received December 9, 2015. This work is supported by the Guangdong Natural Science Funds for Distinguished Young Scholar (S2013050014223), the Shenzhen Development and Reform Commission Funds (55210930-3), the Shenzhen Science, Technology and Innovation Commission Funds (KQCX2015033110182368), and SUSTech Internal Grants (FRG-SUSTC1501A-49, and FRG-SUSTC1501A-63).

Y. Liu and Y. Chen are with the Department of Electrical and Electronic Engineering, South University of Science and Technology, Shenzhen, China.

H. Lin is with Jinghong Communication Technology Co., Ltd., Shanghai, China.

F. H. Juwono is with the School of Electrical, Electronic, and Computer Engineering, University of Western Australia, Perth, Australia, and also with the Department of Electrical Engineering, University of Indonesia, Depok, Indonesia.

This article has been accepted for publication in a future issue of this journal, but has not been fully edited. Content may change prior to final publication. Citation information: DOI 10.1109/LAWP.2016.2536735, IEEE Antennas and Wireless Propagation Letters

lengthens the current path at the ISM band. A stub ST=4.8 mm is loaded to the strip F-H to tune the resonant frequency range at the ISM band. The symmetrically meandered strip with shorting pins is fed in equal amplitude and 180° out of phase to excite the odd mode.

The mixed mode matrix [S] is employed to characterize the differential antenna [8]. The odd mode reflection coefficient is expressed as

$$S_{dd11} = S_{11} - S_{12} \quad (1)$$

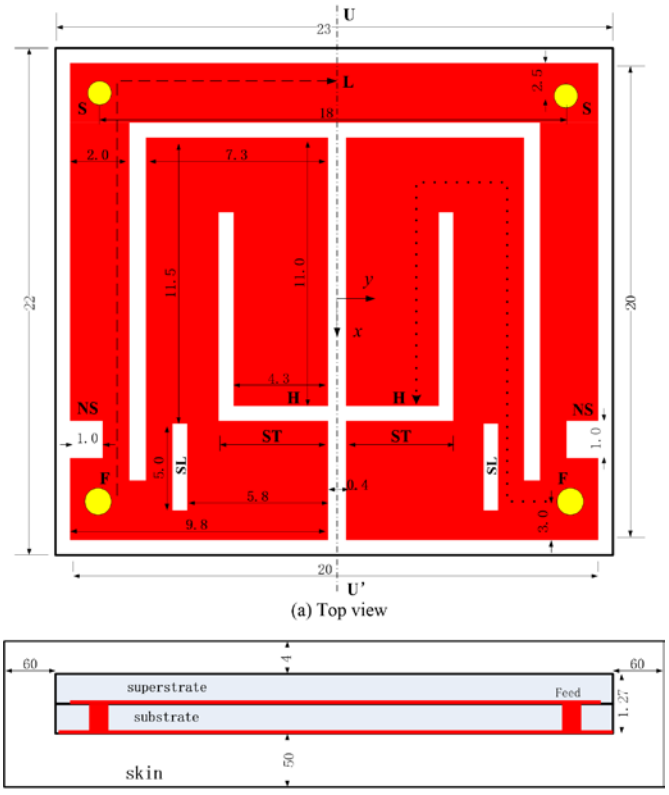

(a) Top view

(b) Side view

Fig. 1. Geometry of the proposed stub-loaded dual-band implantable antenna (unit: mm): (a) top view (b) side view. The strips F-L and F-H are indicated in (a) by using a dashed line and a dotted line, respectively.

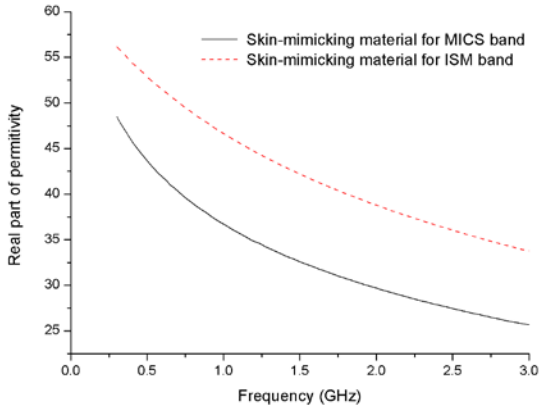

(a) Permittivity of skin-mimicking material at MICS and ISM bands

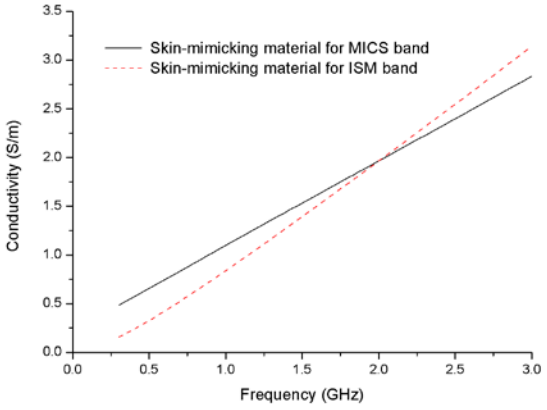

(b) Conductivity of skin-mimicking material at MICS and ISM bands

Fig.2. Measured dielectric properties of skin-mimicking material.

The differentially fed surface electric currents on the strip are shown in Fig. 3. At both 402 MHz and 2400 MHz, the current flows from the left H point to the right H point, and its amplitude is symmetrically distributed about the line UU′. This shows that the odd mode is excited by the differential feed. The current flows along the strip F-H and the stub ST with much lower amplitude than the current along the strip F-L at 402 MHz, which implies that the strip F-L with shorting pin is employed to excite resonance at the MICS band, while the strip F-H and the stub ST have little effect at this band. On the other hand, the current mostly flows on the strip F-H at 2400 MHz, which indicates that the strip F-H plays the key role as a resonator at the ISM band, and the stub ST just tunes the resonance to improve the bandwidth. The symmetrical notches NS and slots SL lengthen the current path to decrease the resonant frequency at the MICS and ISM band, respectively.

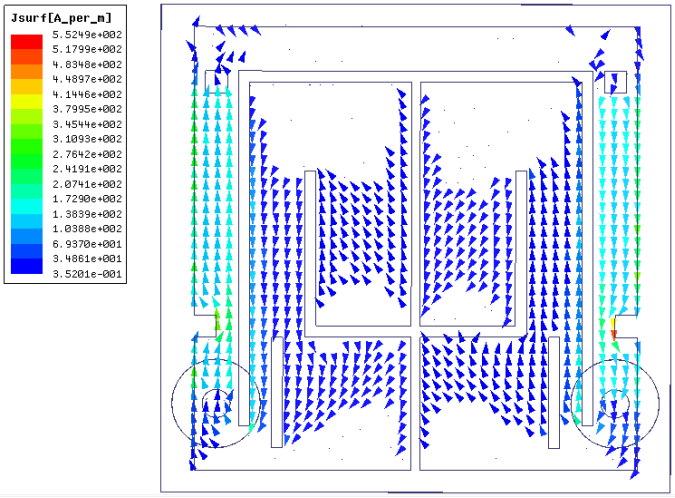

(a) 402 MHz

This article has been accepted for publication in a future issue of this journal, but has not been fully edited. Content may change prior to final publication. Citation information: DOI 10.1109/LAWP.2016.2536735, IEEE Antennas and Wireless Propagation Letters

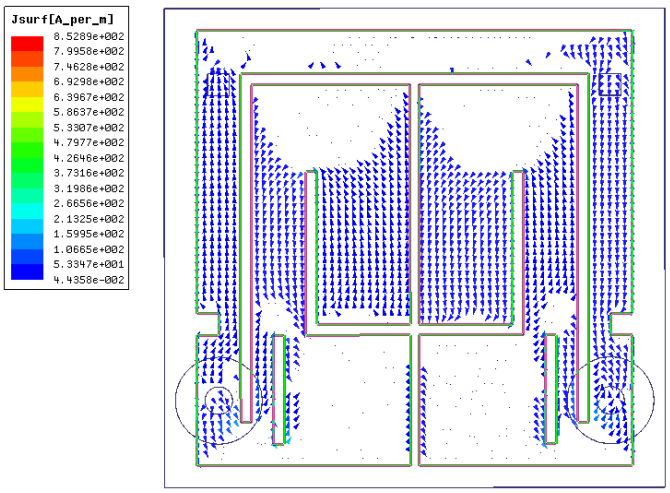

(b) 2400 MHz

Fig. 3. Differentially fed surface electric current distributions at (a) 402 MHz and (b) 2400MHz.

III. Measured Results

The fabricated antenna is shown in Fig. 4(a), which was assembled and embedded into the skin-mimicking material. An Agilent four-port vector network analyzer was used to measure the reflection coefficient of the odd mode, as shown in Fig. 4(b).

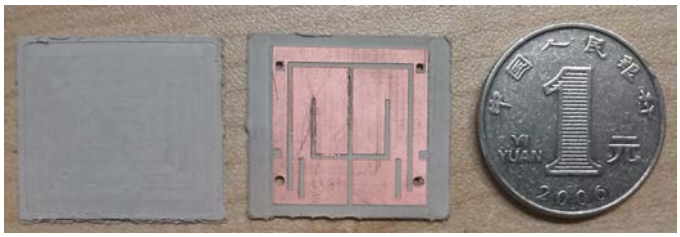

(a) Photograph of the fabricated antenna

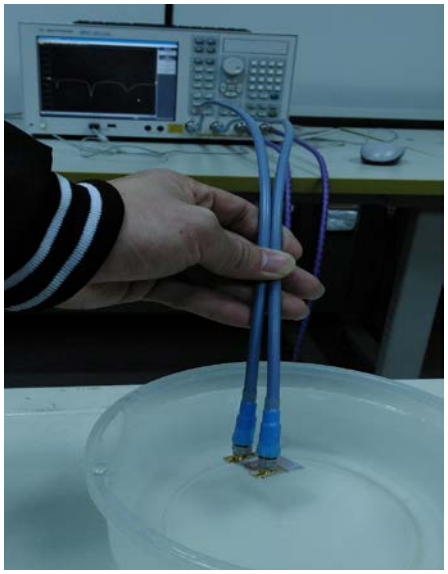

(b) Measurement setup

Fig. 4. (a) Photograph of the fabricated differentially fed implantable antenna and (b) the measurement setup.

Fig. 5 shows the simulated and measured odd mode reflection coefficients of the fabricated antenna inserted into the skin-mimicking materials. The measured 10-dB S_{dd11} bandwidth is 389-419 MHz (7.4%) and 2395-2563 MHz (6.6%), respectively. A slight shift of frequency range occurs. The discrepancy is caused by the fabrication tolerance.

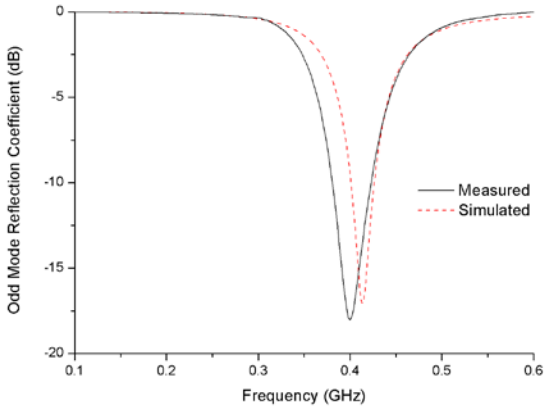

(a) MICS band

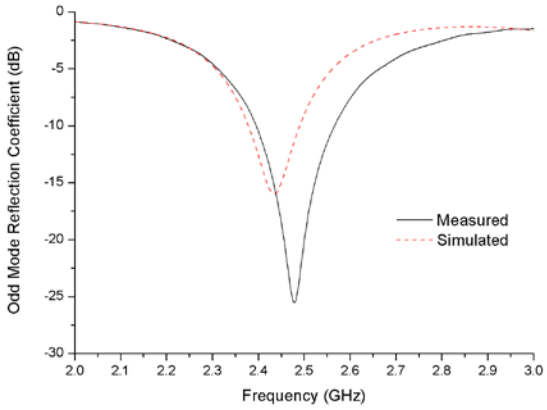

(b) ISM band

Fig. 5. Simulated and measured odd mode reflection coefficients at (a) MICS band and (b) ISM band.

The measured dielectric data were imported into the simulating tool. The simulated far-field gains are -36.7 dBi at 402 MHz and -27.1 dBi at 2400 MHz, respectively, and the simulated cross polarization discriminations (XPD) in the boresight direction are 34.9 dB at 402 MHz and 35.7 dB at 2400 MHz, respectively. Gains are lower than those in the existing literatures, because the dielectric data employed in the simulations are based on the measurement setting, which are different from those used previously and the antenna was embedded in the lossy medium, not in free space. Due to the quite low gains, this prototype is more suitable for near-field communication in biotelemetry applications, where the near-field boundary is $\lambda/2\pi$ [9]. In view of the use scenario, the

This article has been accepted for publication in a future issue of this journal, but has not been fully edited. Content may change prior to final publication. Citation information: DOI 10.1109/LAWP.2016.2536735, IEEE Antennas and Wireless Propagation Letters

far-field measurement of the radiation pattern may not provide very relevant information about the antenna performance due to the different patterns between near- and far-field regions [9]. Instead, an external half-wavelength dipole was placed close to the implantable antenna embedded in the skin-mimicking material to evaluate the coupling strength. The setup is shown in Fig. 6, and the simulated coupling strength is given in Fig. 7. The coupling at the ISM band is higher than that at the MICS band due to larger gains at the ISM band.

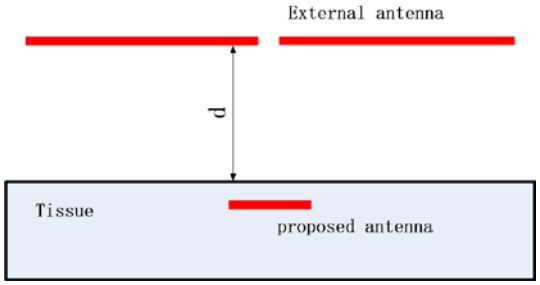

Fig.6. Setup for coupling strength evaluation.

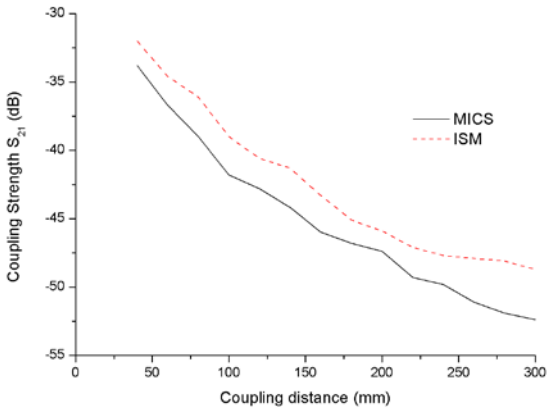

Fig. 7. Simulated coupling strength for external half-wavelength dipole.

When the designed antenna is assumed to deliver a differential power of 1 W (i.e., input 1 W at one port and input 1 W at the other port with 180° out of phase), the simulated maximum 1-g averaged SAR values are shown in Table I. When the delivered power is below 3.8 mW and 4.6 mW for the MICS and ISM bands, respectively, the SAR regulation of ANSI/IEEE (1.6 W/kg) [10] can be satisfied.

TABLE I
SIMULATED 1-G AVERAGED MAXIMUM SAR (INPUT DIFFERENTIAL POWER =1W)

Frequency (MHz)	1-g Averaged Maximum SAR (W/kg)	Maximum Input Differential Power (mW)
402	832	3.8
2400	690	4.6

IV. CONCLUSION

A differentially fed compact dual-band implantable antenna has been presented, where the symmetrically meandered strip with symmetrically located shorting pin was employed for the odd mode excitation. The measured 10-dB odd mode reflection coefficient bandwidth is 7.4% at the MICS band and 6.6% at the ISM band, respectively. Excellent agreement between the simulated and measured results has been observed. The simulated 1-g averaged SAR values have also been presented, which demonstrates that the SAR values comply with the regulation of ANSI/IEEE.

REFERENCES

[1] D. Panescu, "Emerging technologies [wireless communication systems for implantable medical devices]," *IEEE Eng. Med. Bio. Mag.*, vol. 27, no. 2, pp. 96-101, Mar. 2008.

[2] T. Karacolak, A. Z. Hood and E. Topsakal, "Design of a dual-band implantable antenna and development of skin mimicking gels for continuous glucose monitoring," *IEEE Trans. Microw. Theory Tech.*, vol. 56, no. 4, pp. 1001-1008, Apr. 2008.

[3] P. C. M. Soontornpipit and C. C. You, "Design of implantable microstrip antenna for communication with medical implants," *IEEE Trans. Microw. Theory Tech.*, vol. 52, no. 8, pp. 1944-1951, Aug. 2004.

[4] W.R. Deal, V. Radisic, Y. Qian, and T. Itoh, "Integrated-antenna push-pull power amplifiers," *IEEE Trans. Microw. Theory Tech.*, vol. 47, no. 8, pp. 1418-1425, Aug. 1999.

[5] Z. Duan, Y.-X. Guo, R.-F. Xue, and D.-L. Kwong, "Differentially fed dual-band implantable antenna for biomedical applications," *IEEE Trans. Antennas Propagat.*, vol. 60, no. 12, pp. 5587-5595, Dec. 2012.

[6] Z. Duan, Y.-X. Guo, Minkyu Je, and D.-L. Kwong, "Design and in vitro test of a differentially fed dual-band implantable antenna operating at MICS and ISM bands," *IEEE Trans. Antennas Propagat.*, vol. 62, no. 5, pp. 2430-2439, May 2014

[7] T. S. P. See, X. Qing, W. Liu and Z. N. Chen, "A wideband ultra-thin differential loop-fed patch antenna for head implants," *IEEE Trans. Antennas Propagat.*, vol. 63, no.7, pp. 3244-3248, July 2015

[8] D. E. Bockelman and W. R. Eisenstadt, "Combined differential and common-mode scattering parameters: Theory and simulation," *IEEE Trans. Microw. Theory Tech.*, vol. 43, no. 7, pp. 1530-1539, Jul. 1995

[9] J. D. Kraus, "Antenna Measurements," in *Antennas for All Applications*, 3rd ed., McGraw-Hill, 2002

[10] *IEEE Standard for Safety Levels with respect to Human Exposure to Radio Frequency Electromagnetic Fields, 3 KHz to 300 GHz*, IEEE Standard C95.1-2005, 2005.